Deuterium site occupancy and phase boundaries in $ZrNiD_x$ $(0.87 \leq x \leq 3.0)$

R. C. Bowman, Jr.,[1,*] Natalie L. Adolphi,[2] Son-Jong Hwang,[3] J. G. Kulleck,[1] T. J. Udovic,[4] Q. Huang,[4] and H. Wu[4,5]
[1]*Jet Propulsion Laboratory, California Institute of Technology, Pasadena, California 91109, USA*
[2]*New Mexico Resonance, Albuquerque, New Mexico 87106, USA*
[3]*The Division of Chemistry and Chemical Engineering, California Institute of Technology, Pasadena, California 91125, USA*
[4]*NIST Center for Neutron Research, National Institute of Standards and Technology, Gaithersburg, Maryland 20899-8562, USA*
[5]*Department of Materials Science and Engineering, University of Maryland, College Park, Maryland 20742-2115, USA*
(Received 7 June 2006; revised manuscript received 18 August 2006; published 8 November 2006)

$ZrNiD_x$ samples with compositions between $x=0.87$ and $x=3.0$ were investigated by ^2H magic-angle spinning nuclear magnetic resonance spectroscopy (MAS-NMR), powder x-ray diffraction (XRD), neutron vibrational spectroscopy (NVS), and neutron powder diffraction (NPD). The rigid-lattice MAS-NMR spectrum for a $ZrNiD_{0.88}$ sample in the triclinic β phase shows a single phase with two well-resolved resonances at +11.5 and −1.7 ppm, indicating that two inequivalent D sites are occupied, as was observed previously in $ZrNiD_{1.0}$. For $ZrNiD_{0.88}$, the ratio of spectral intensities of the two lines is 1:0.76, indicating that the D site corresponding to the +11.5 ppm line has the lower site energy and is fully occupied. Similarly, the neutron vibrational spectra for $ZrNiD_{0.88}$ clearly confirm that at least two sites are occupied. For $ZrNiD_{1.0}$, XRD indicates that ~5% of the metal atoms are in the γ phase, corresponding to an upper composition for the β phase of $x=0.90\pm0.04$, consistent with the MAS-NMR and neutron vibrational spectra indicating that $x=0.88$ is single phase. The MAS-NMR and NVS of $ZrNiD_{1.87}$ indicate a mixed-phase sample ($\beta+\gamma$) and clearly show that the two inequivalent sites observed at $x=0.88$ cannot be attributed to the sites normally occupied in the γ phase. For $ZrNiD_{2.75}$, NPD results indicate a γ-phase boundary of $x=2.86\pm0.03$ at 300 K, increasing to 2.93 ± 0.02 at 180 K and below, in general agreement with the phase boundary estimated from the NVS and MAS-NMR spectra of $ZrNiD_{1.87}$. Rigid-lattice ^2H MAS-NMR spectra of $ZrNiD_{2.75}$ and $ZrNiD_{2.99}$ show a ratio of spectral intensities of $1.8\pm0.1:1$ and $2.1\pm0.1:1$ ($Zr_3Ni:Zr_3Ni_2$), respectively, indicating complete occupancy of the lower-energy Zr_3Ni_2 site, consistent with the NPD results. For each composition, the correlation time for deuterium hopping was determined at the temperature where resolved peaks in the MAS-NMR spectrum coalesce due to motion between inequivalent D sites. The measured correlation times are consistent with previously determined motional parameters for $ZrNiH_x$.

DOI: 10.1103/PhysRevB.74.184109 PACS number(s): 61.10.Nz, 76.60.Cq, 66.30.Fq, 78.70.Nx

I. INTRODUCTION

The $ZrNiH_x$ system was among the first intermetallic hydride systems to be prepared[1] and has been the subject of a number of studies of its crystal structure,[2–5] interstitial site occupancy,[4,6–11] thermodynamic properties,[1,11–15] and electronic structure.[16,17] The compound has also been favorably evaluated for a number of technological applications including tritium handling and storage,[12,18,19] closed-cycle Joule-Thomson cryogenic refrigerators that form solid H_2 at ~10 K,[20,21] and reversible gas-gap thermal switches.[22]

The structure of ZrNi metal is orthorhombic (space group *Cmcm*), and the metal sublattice retains essentially the same structure during the formation of the γ-phase hydride $ZrNiH_x$ with a hydrogen content of $x\sim3$.[2–4] $ZrNiH_x$ also forms a stable intermediate hydride (i.e., the β phase) at $x\sim1$ (Refs. 4 and 11) with H occupying the interstitial site that has been often referred to as Zr_4 (Ref. 6). We note this site is better described[23] as having six nearest neighbors (4 Zr atoms and 2 Ni atoms at M-H distances of 2.30 and 2.32 Å, respectively), and we will hence refer to this site as Zr_4Ni_2. There is one Zr_4Ni_2 site per ZrNi, and previous x-ray and neutron-diffraction measurements[4] indicated that only this site is occupied in the β phase, which exists as a single nonstoichiometric phase for $0.65<x<1.0$ at $T\geq320$ K.[11] The ZrNi lattice in the β phase reportedly[4,16] exhibits a slight triclinic distortion of the host structure. For γ-phase $ZrNiD_3$, a number of previous measurements[3,8,10] indicate that two inequivalent deuterium (hydrogen) sites—tetrahedral Zr_3Ni sites (2 per ZrNi) and pyramidal Zr_3Ni_2 sites (1 per ZrNi)—are occupied.[6] The nominal trihydride γ-$ZrNiH_x$ has been reported[4,11,16] to be single phase for $\sim2.5<x<3.0$ above room temperature. Electronic structure calculations also support the occupation of Zr_4Ni_2 sites in the monohydride β phase and the occupation of Zr_3Ni and Zr_3Ni_2 sites in the trihydride γ phase, which result in the lowest total energies for these two phases.[16,17]

While there is general agreement regarding the H- (or D-) site occupancy in the γ phase, there remain some questions regarding site occupancy in the β phase. Although several studies conclude that the Zr_4Ni_2 sites are the only sites occupied in the β phase,[4,6,16,17] other work[7–10] indicates that as many as three different H (D) sites are occupied in $ZrNiH(D)_x$ samples for $0.5<x<1.0$.

In a previous NMR study of $ZrNiD_x$ phases by Adolphi *et al.*,[10] the ^2H MAS-NMR spectrum of $ZrNiD_{3.0}$ (γ phase) showed two inequivalent D sites with a 2:1 ratio of intensities in agreement with previous observations.[3,4,8] The ^2H MAS-NMR spectra of $ZrNiD_{1.0}$ (nominally β phase) indicated that three different sites were occupied in two different phases.[10] The spectrum of the dominant phase (~80% of D atoms), assumed to be the β phase, consisted of two well-

resolved resonances with a nearly 1:1 ratio of intensities. These two resonances were clearly different (in line shape, center frequency, and temperature dependence) from the resonances observed in the spectrum of the γ-phase sample. Therefore, it was proposed that the two inequivalent sites occupied in the β phase are attributable to two distinct off-center positions within the large Zr_4Ni_2 sites, related to the triclinic distortion of the orthorhombic lattice. The third resonance observed in the spectrum of $ZrNiD_{1.0}$ ($\sim$20% of the D atoms) was assumed to be in a different phase due to its different T_1. This secondary phase could not be definitely identified, but was assumed to be the γ phase.[10]

The occupancy of three inequivalent sites was also observed in an inelastic neutron-scattering study[8] and a Mössbauer spectroscopy study[9] in $ZrNiH_x$ samples with concentrations $0.5<x<1.0$. In these studies, the spectral components were assumed to correspond to the *A*, *B*, and *C* sites (i.e., "Zr_4," Zr_3Ni, and Zr_3Ni_2) previously identified by Westlake.[4,6] Neither study considered the possibility of more than one H position within nominally the same site (i.e., the aforementioned distorted Zr_4Ni_2 location). In the low-resolution neutron vibrational spectroscopy (NVS) study by Benham *et al.*,[8] the apparent occupancy of *B* and *C* sites was attributed to two-phase coexistence ($\beta+\gamma$ phases), assuming a very large shift of phase boundaries toward the lower concentration at 80 K. In contrast, from their Mössbauer study of ^{57}Fe-doped $ZrNiH_x$, Yang *et al.*,[9] suggested that all three occupied sites are in the same β phase.

The present study was undertaken to clarify the deuterium site occupancy and phase boundaries for β-$ZrNiD_x$. We hence prepared two new concentrations, $x=0.88$ and $x=1.87$, and investigated them in greater detail using ^{2}H MAS-NMR, NVS, NPD, and x-ray diffraction. The $x=0.88$ sample is shown to be single β phase, while the $x=1.87$ sample is a mixture of the β and γ phases.[4,11–17] These MAS-NMR and NVS spectra confirm that deuterium atoms occupy two inequivalent interstitial sites in the β phase. Moreover, we present MAS-NMR, NVS, and NPD results for additional $ZrNiD_x$ samples with $2.5<x<3.0$ to determine the lower composition boundary for the nonstoichiometric γ phase.

II. EXPERIMENTAL SECTION

All $ZrNiH_x$ and $ZrNiD_x$ samples examined during the present NMR and XRD studies were prepared by gas-phase reactions between very high-purity hydrogen and deuterium gas, respectively, with pieces cut from a single large (i.e., $\sim$400 g) ingot of high-purity ZrNi intermetallic alloy originally produced by the Teledyne Wah Chang Company[24] (Albany, OR 97321, USA) using a crystal-bar purity Zr and Ni metal of comparable purity. The measured composition of this ingot matched the ideal Zr/Ni ratio of 1.00 ± 0.01. Detailed microscopic and x-ray-diffraction examinations have been performed by Michel *et al.*[16] on another piece taken from this same ZrNi ingot. They reported the material was almost completely the orthorhombic ZrNi phase with a high density of twinning defects and a minor secondary phase of composition Zr_9Ni_{11}, which lies along the grain boundaries of the host matrix. Chemical analyses on this ZrNi ingot gave the following impurities by weight: Fe (130 ppm), O (72 ppm), C (70 ppm), Cu (48 ppm), Mn (23 ppm), N (7 ppm), and no other elements were detected. Other portions of this same ZrNi ingot were also used by (1) Dantzer *et al.*[15] to obtain the hydrogen absorption and desorption isotherms at 483 K and 499 K for their sample #2; (2) Prina *et al.*[22] for the preparation and cycling of gas gap heat switches using $ZrNiH_x$; (3) Adolphi *et al.*,[10] for their prior NMR experiments on $ZrNiD_{1.0}$ and $ZrNiD_{3.0}$; and Browning *et al.*[25] for NMR relaxation-times studies of diffusion in the β and γ phases.

Most of the deuteride (hydride) samples investigated in this paper were prepared at the Jet Propulsion Laboratory (and are denoted as JPL) in an all-metal Sieverts volumetric system constructed from electropolished 316*L* stainless-steel tubing and components using the procedures described in greater detail elsewhere.[25] After each reaction, the closed reactor vessel was removed from the Sieverts manifold to be opened under a purified argon atmosphere in a glove box for removing the now brittle products, which were ground in an agate mortar and pestle until all material passed through a 200-mesh sieve yielding powders with dimensions smaller than 75 μm. Properties of all $ZrNi(H/D)_x$ samples used in the present NMR, XRD, and NVS experiments along with information on the $ZrNiD_{1.0}$ and $ZrNiD_{3.0}$ previously prepared and studied by Adolphi *et al.*,[10] are summarized in Table I. The listed compositions are based upon volumetric determinations of the H_2 (or D_2) gas absorbed during the final reaction step for each sample. Comparison with mass changes following reactions indicate these compositions give *x* values accurate within ±0.02.

In order to establish the phase compositions of all the samples in Table I, powder XRD measurements[22,25] were performed at room temperature using a Siemens D500 diffractometer operating with copper K_α radiation. Each $ZrNi(H/D)_x$ sample was mixed with a small amount of crystalline silicon powder as an internal reference material and placed in a cell with a thin window of Kapton film to reduce scattering background. Depending upon stoichiometry and isotope content, essentially all of the XRD peaks for each material in Table I could be assigned to one of the following phases from the International Center for Diffraction Data [Newtown Square, PA 19073-3273, USA] JCPDS files: α-ZrNi (No. 50-1095); β-$ZrNiH_{1.0}$ (No. 50-1096); β-$ZrNiD_{1.0}$ (No. 50-1098); γ-$ZrNiH_{2.7}$ (No. 50-1097); or γ-$ZrNiD_{2.7}$ (No. 50-1099). However, better fits to the β-phase spectra were obtained using a different triclinic unit cell for space group No. $P1(1)$, as described in the results section. Only sample JPL-06 (i.e., $ZrNiD_{1.87}$) indicated a mixture of the $\beta+\gamma$ phases from the XRD results. As expected from the earlier results of Michel *et al.*[16] on samples from the same ingot, the present XRD patterns for the ZrNi powder (JPL-02) and β-phase hydrides/deuterides contained some weak peaks (i.e., $\leq$2 wt %) attributable to the Zr_9Ni_{11} intermetallic (i.e., JCPDS file No. 33-0963) as an impurity phase. These Zr_9Ni_{11} XRD peaks were shifted to slightly lower angles for the γ-phase samples, which is consistent with lattice expansion upon deuterium absorption to form a solid solution $Zr_9Ni_{11}D_x$ phase.[26] However, any more detailed assessment

TABLE I. Summary of the $ZrNiD_x$ and $ZrNiH_{0.88}$ samples prepared for MAS-NMR and neutron-scattering experiments with phase identifications and lattice parameters at room temperature from powder XRD. The widely accepted orthorhombic structure (*Cmcm*) was used to obtain the α- and γ-phase parameters. For the β phase, XRD and NPD data are in agreement with a new triclinic type $P1$ (No. 1) space group with the lattice parameters determined from NPD data for $ZrNiD_{0.88}$ included, along with fits to the XRD patterns for all samples.

Composition	ID (Ref.)	Major phase	a (Å)	b (Å)	c (Å)	Unit-cell volume (Å^3)	Other phases seen
$ZrNiD_{3.00}$	JPL-13	γ	3.528(2)	10.470(5)	4.303(2)	158.9(3)	$Zr_9Ni_{11}D_x$ (~1–2 %)
$ZrNiD_{2.99}$	Knox-5	γ	3.526(1)	10.469(2)	4.297(2)	158.6(1)	$Zr_9Ni_{11}D_x$ (~1–2 %)
$ZrNiD_{2.75}$	NIST-275	γ	3.525(3)	10.484(9)	4.290(5)	158.5(5)	$Zr_9Ni_{11}D_x$
$ZrNiD_{2.64}$	JPL-05	γ	3.518(2)	10.470(6)	4.278(3)	157.6(5)	$Zr_9Ni_{11}D_x$
$ZrNiD_{1.87}$	JPL-06	γ	3.522(7)	10.48(3)	4.272(13)	157.6(12)	$Zr_9Ni_{11}D_x$
		β	5.276(6) (101.67°)	5.391(8) (100.60°)	5.233(5) (100.69°)	139.4(3)	
$ZrNiD_{1.00}$	Knox-1	β	5.264(4) (101.63°)	5.386(4) (100.70°)	5.228(3) (100.62°)	138.8(2)	$Zr_9Ni_{11}D_x$ (~1%) + γ phase (~5%)
$ZrNiD_{0.88}$ (XRD)	JPL-14	β	5.269(5) (101.63°)	5.377(6) (100.60°)	5.239(5) (100.72°)	139.0(4)	Zr_9Ni_{11} No γ phase
$ZrNiD_{0.88}$ (NPD)	JPL-14	β	5.264(1) (101.52°)	5.375(1) (100.66°)	5.226(1) (100.59°)	138.6(1)	Zr_9Ni_{11}, ZrNi
$ZrNiD_{0.87}$	JPL-07	β	5.266(4) (101.55°)	5.370(4) (100.74°)	5.222(4) (100.60°)	138.3(3)	Zr_9Ni_{11} No γ phase
$ZrNiH_{0.88}$	JPL-18	β	5.270(6) (101.67°)	5.372(6) (100.65°)	5.238(6) (100.71°)	138.9(4)	Zr_9Ni_{11} No γ phase
ZrNi	JPL-02	α	3.262(7)	9.972(33)	4.103(9)	133.5(7)	Zr_9Ni_{11} (~1–2 %)

is impossible from the very few and weak peaks for these latter phases. Although this very low amount of the $Zr_9Ni_{11}D_x$ was not expected to have any significant influence on the deuterium-site occupancies for the dominant β- and γ-$ZrNiD_x$ phases in these samples, our inability to determine accurately the $Zr_9Ni_{11}D_x$ stoichiometry did increase the uncertainty during the NMR and NVS evaluations of the phase boundaries. None of the XRD patterns indicate the presence of binary ZrH_x, zirconium oxides, or other Zr-Ni intermetallic phases for any of the samples listed in Table I.

In a high-resolution solid-state NMR ^{2}H spectrum, each inequivalent deuterium nucleus generally has a different NMR frequency while the area of each spectral component is proportional to the number of nuclei at that frequency. Provided that these spectral features are sufficiently well resolved, interpretation of these ^{2}H spectra can be very straightforward as was demonstrated with YD_x by Adolphi *et al.*[27] As described previously,[10] magic-angle spinning (MAS) ^{2}H NMR spectra were obtained at 4.7 T (f_0=30.85 MHz) using a rotor-synchronized Hahn Echo sequence ($\pi/2_x - t - \pi_y$), with t chosen to be an integer number of MAS rotor periods,[28] and now also at 11.7 T (76.79 MHz) using a single 6 μs-$\pi/2$ pulse. The NMR frequency shifts are referenced to D_2O with an estimated uncertainty of ±0.2 ppm, based upon reproducibility of the measurements. In the 30.85 MHz spectra, the relative uncertainty in the sample temperatures is ±1 K, while the absolute temperature uncertainty is ±5 K, as described in Ref. 10. In the 76.79 MHz spectra, about 200 mg of powder mixture ($ZrNiD_x$ + $Pb(NO_3)_2$ + SiO_2 with a rough ratio of 40:30:30 wt %) was spun at ~6 kHz for ^{2}H variable temperature MAS experiments using a Bruker 4 mm double-resonance probe while the ^{207}Pb MAS NMR signal was first measured, to determine the temperature, after thermal equilibrium at each temperature. The temperature range was 174–377 K. The temperature of the probe was calibrated using a $Pb(NO_3)_2$ powder employing a well-established procedure[29,30] and the accuracy is ±1 K. From the full width at the half maximum of the ^{207}Pb MAS signal, it was estimated that temperature gradients across these latter variable-temperature samples in the Bruker probe were as large as 4.9 K.

Both neutron powder diffraction (NPD) and neutron vibrational spectroscopy (NVS) experiments were undertaken at the NIST Center for Neutron Research. Samples of β-phase $ZrNiD_{0.88}$ and $ZrNiH_{0.88}$ were prepared at JPL and are identified in Table I as JPL-14 and JPL-18, respectively. Different $ZrNiD_x$ stoichiometries (i.e., ~0.0, 1.87, 2.5, 2.75, and 3.0) were also synthesized at NIST in sequence from the JPL-14 sample using a Sieverts apparatus after completion of the NVS and NPD experiments with x=0.88. Typically, the $ZrNiD_x$ sample was heated to ~673 K to desorb the initial deuterium content followed by deuterium absorption from a known volume during a slow overnight cool down to room temperature to obtain the other compositions. These $ZrNiD_x$ (x=0.88, 1.87, 2.5, 2.75, and ~3.0) samples (~23 g) and the $ZrNiH_{0.88}$ sample JPL-18 (≈4.8 g) were used in the NVS measurements, which were performed with the BT-4 filter-

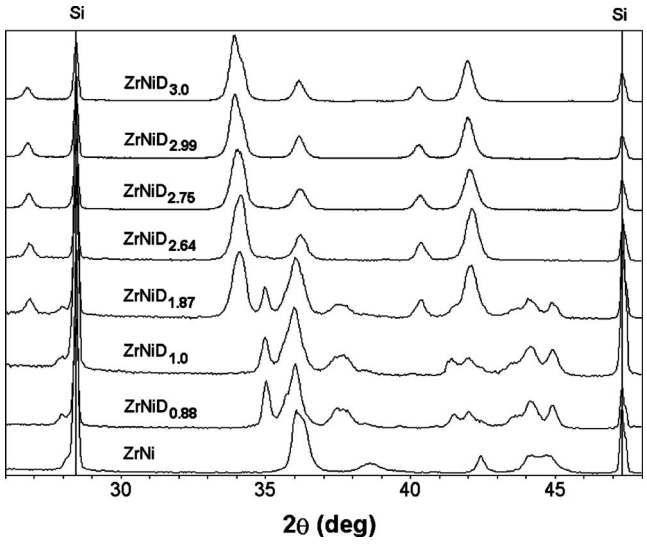

FIG. 1. Portions of powder x-ray-diffraction (XRD) patterns for eight $ZrNiD_x$ compositions at $x=0.0$ [JPL-02], 0.88 [JPL-14], 1.00 [Knox-1], 1.87 [JPL-06], 2.64 [JPL-05], 2.75 [NIST-275], 2.99 [Knox-5], and $x=3.00$ [JPL-13]. The solid vertical lines mark the two XRD peaks for the silicon (Si) powder reference.

analyzer neutron spectrometer[31] using the Cu(220) monochromator. The horizontal divergences were 20′ of arc for both the in-pile and monochromatic-beam collimators. The low-bandpass filter analyzer consists of a composite Bi/Be/graphite/Be filter, which yields an average neutron final energy of ≈1.2 meV.

The NPD measurements were performed with the BT-1 high-resolution powder diffractometer[32] using the Cu(311) monochromator at a wavelength of 1.5401(1) Å. The horizontal divergences were 15′, 20′, and 7′ of arc for the in-pile, monochromatic-beam, and diffracted-beam collimators, respectively. Data were collected every 0.05° over a 2θ angular range of 3 to 160°. All refinements were carried out with the Rietveld method[33] using the program GSAS.[34] Neutron-scattering amplitudes used in the refinements were 7.16, 10.3, and 6.67 fm for Zr, Ni, and D, respectively.[34]

III. RESULTS AND DISCUSSION

A. X-ray diffraction

Representative x-ray diffraction (XRD) patterns for eight $ZrNiD_x$ samples with $x=0.0$, 0.88, 1.0, 1.87, 2.64, 2.75, 2.99, and 3.0 are shown in Fig. 1. Table I lists the lattice parameters and phase identifications from the XRD measurements for most of the $ZrNiD_x$ samples that were prepared for NMR and neutron-scattering studies. The lattice parameters for each sample have been assigned to one of the three known $ZrNi(H/D)_x$ phases (i.e., orthorhombic α phase, triclinic β phase, and orthorhombic γ phase) to obtain "best fits." There is only one clearly identified impurity phase (i.e., Zr_9Ni_{11} intermetallic, which has its two weakly observable XRD peaks for this ZrNi alloy at 39.7° and 40.8° that shifted to lower angles—presumably from an expanded isostructural hydride phase, for $x > \sim 2.0$) at a content of ~2% in these patterns. Michel *et al.*,[16] have previously reported about the same amount of this impurity phase being in the grain boundaries of their samples prepared from another portion of this ZrNi ingot. So, detection of small amounts of this impurity in the present XRD patterns is not a surprise.

For $ZrNiD_{1.0}$, the fit of the XRD pattern indicates that approximately 5±1% of the metal atoms are in the γ phase. This result implies that the upper β-phase boundary is $x=0.90\pm0.04$, assuming that the lower γ-phase boundary lies anywhere within the range $x=2.5-3.0$. In the MAS-NMR spectrum of $x=1.0$ (Ref. 10), an unidentified secondary phase was observed that accounted for ~20% of the D atoms in the sample. Assuming that the secondary phase was the γ phase, one estimates an upper phase boundary for the β phase of $x \approx 0.87$, in good agreement with the phase boundary determined here from XRD.

Although all the peaks in these XRD patterns that are attributable to the α phase or γ phase have been consistently assigned with reasonable lattice parameters and fits, we could not get consistent results for the triclinic β-phase samples with $x \sim 0.9-1.0$ using the previously reported JCPDS Ref. No. 50-1096 or No. 50-1098 parameters, since several significant peaks would not index properly. All the peaks in the current β-phase XRD patterns could be indexed using a different triclinic unit cell for space group $P1$ (No. 1) that was also determined from the NPD pattern measured for $ZrNiD_{0.88}$ (discussed later), with lattice parameters given in Table I. With lattice angles over 10° larger than 90°, it is possible that the β-phase structure is much more distorted than previously suggested[4,6] with multiple lower-symmetry H/D sites, which might also account for the two peaks in ^{2}H MAS-NMR spectra.[10] These new parameters for β phases with $P1$ symmetry have also been obtained from the XRD patterns and are given in Table I. While the atomic positions comprising the actual β-phase structure are still unknown awaiting a successful detailed Rietveld refinement analysis of the NPD data, all the XRD patterns for the β-phase samples appear to match this specific space group.

B. NMR-$ZrNiD_{1.87}$

The open circles in Fig. 2 are the fully relaxed, rigid lattice ^{2}H MAS-NMR spectrum of $ZrNiD_{1.87}$ at 163 K. Three resonances (with Knight/chemical shifts of roughly +10, −4, and −12 ppm relative to D_2O) are clearly resolved. Spinning sidebands occur at integral multiples of the MAS rotor frequency (8.0 kHz) centered about each resonance. The solid line is a fit to the data assuming a linear combination of the β- and γ-phase spectra. In the fit, the β-phase spectrum (dashed line in the inset) was assumed to have two lines with the same Gaussian shape, sideband intensities, splitting (13.4 ppm), and ratio of intensities (1:1) as were observed previously for $ZrNiD_{1.0}$.[10] Similarly, the γ-phase spectrum (dotted line in the inset) was assumed to have two lines with the same Lorentzian shape, sideband intensities, and splitting (19.6 ppm) observed previously in the spectrum of $ZrNiD_{3.0}$. The intensity ratios of the two lines in the γ-phase spectrum, the center frequencies of the β- and γ-phase spectra, and the intensities of the two phases were allowed to vary. The fit

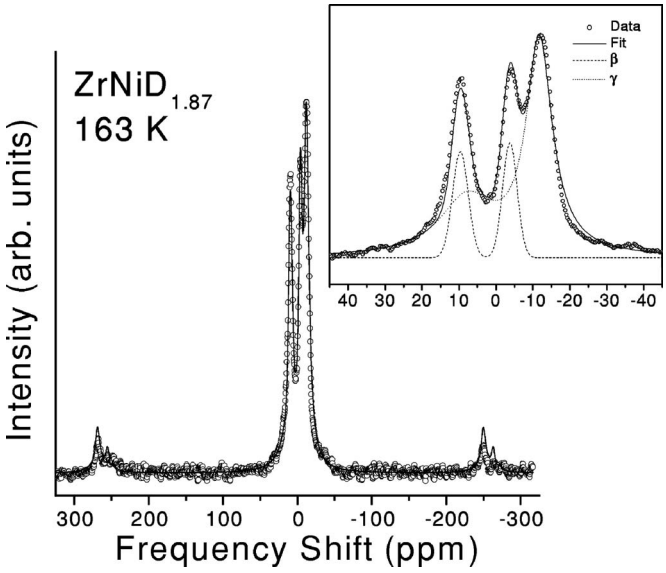

FIG. 2. Rigid-lattice ^{2}H MAS-NMR spectrum (f_0=30.85 MHz) of $ZrNiD_{1.87}$ (open circles). Spinning sidebands are evident at ±8 kHz (±259 ppm). The inset shows an expanded view of the centerband. The fit to the spectrum (solid line) shows that the sample is a mixture of β phase (dashed line in the inset) and γ phase (dotted line in the inset).

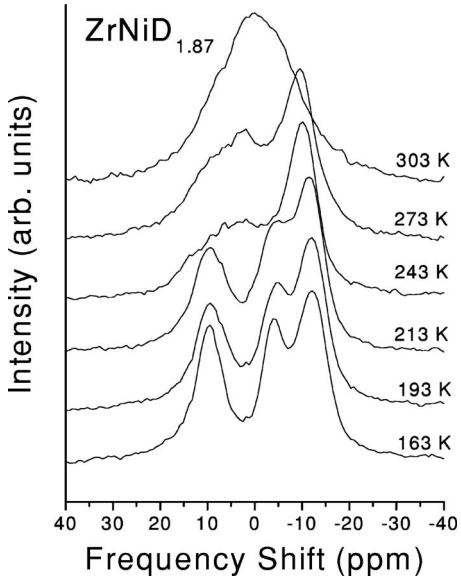

FIG. 3. Temperature dependence of the ^{2}H MAS-NMR spectrum (f_0=30.85 MHz) of $ZrNiD_{1.87}$. As temperature increases, the β-phase lines coalesce between 213 and 243 K due to the increasing rate of deuterium hopping between the two inequivalent sites in that phase. Similarly, the γ-phase lines coalesce between 273 and 303 K.

yielded the following frequency shifts: +9.7 and −3.7 ppm for the β-phase lines, and +7.9 (Zr_3Ni_2 site) and −11.7 (Zr_3Ni site) for the γ-phase lines, which agree within uncertainty with the shifts reported previously[10] for x=1.0 and x=3.0. The MAS-NMR parameters for all the $ZrNiD_x$ previously reported and from the present measurements are collected in Table II. In the $ZrNiD_{1.87}$ spectrum, the γ phase accounts for 78±5 % of the spectral intensity (i.e., 78% of the deuterium in the sample), from which we estimate the γ-phase concentration to be x=2.7±0.3.

The temperature dependence of the ^{2}H MAS-NMR spectrum of $ZrNiD_{1.87}$ (Fig. 3) confirms that the lines at +9.7 and −3.7 arise from the same phase. As the temperature increases, the two resolved resonances at +9.7 and −3.7 coalesce into one line at a temperature somewhere between 213 and 243 K due to exchange (i.e., the hopping of D atoms between the two chemically inequivalent sites). Two separate resonances are observed in the spectrum only when the hopping rate τ_c^{-1} is sufficiently slow compared to the frequency splitting $\Delta\omega$ (i.e., when $\tau_c^{-1} \ll \Delta\omega$), while a single resonance at the average NMR frequency is observed at higher temperatures (where $\tau_c^{-1} \gg \Delta\omega$).[28] At the coalescence temperature,

$$\tau_c^{-1} = \Delta\omega/2. \quad (1)$$

For the β phase in x=1.87, the 13.4 ppm splitting of the β-phase lines is equivalent to 414 Hz, giving a correlation time $\tau_c = 7.7 \times 10^{-4}$ s at ~230 K. This temperature is very similar to the coalescence temperature observed at the same field in $ZrNiD_{1.0}$ (223 K), indicating that the motional parameters in the β phase of the x=1.87 sample are nearly the same as those in the $ZrNiD_{1.0}$ sample, as expected.

TABLE II. Summary of ^{2}H MAS-NMR parameters measured for β-phase and γ-phase $ZrNiD_x$ in this work and Ref. 10.

			^{2}H peaks for β phase			^{2}H peaks for γ phase		
x	NMR frequency (MHz)	T (K)	β_I (ppm)	β_{II} (ppm)	Ratio (I/II)	γ_I (Zr_3Ni) (ppm)	γ_{II} (Zr_3Ni_2) (ppm)	Ratio (I/II)
3.0[a]	30.85	300				−10.1	+9.5	2.1/1.0
2.99	76.79	213				−10.0	+9.6	2.1/1.0
2.75	76.79	180				−10.5	+9.0	1.8/1.0
1.87	30.85	163	−3.7	+9.7	1.0/1.0	−11.7	+7.9	1.2/1.0
1.00[a]	30.85	163	−2.3	+11.1	1.0/1.0			
0.88	76.79	174	−1.7	+11.5	0.76/1.0			

[a]Reference 10.

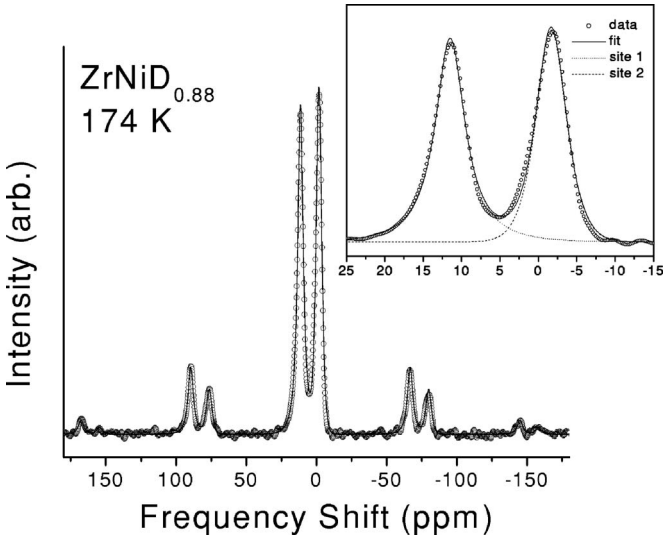

FIG. 4. Rigid-lattice ^{2}H MAS-NMR spectrum (f_0=76.79 MHz) of $ZrNiD_{0.88}$ (open circles). Spinning sidebands are evident at ±6 kHz (±78 ppm). The inset shows an expanded view of the centerband. The fit to the spectrum (solid line) yields a ratio of intensities of the two resonances of 1:0.76 suggesting that the D site corresponding to the higher-frequency resonance (dotted line in inset) is fully occupied.

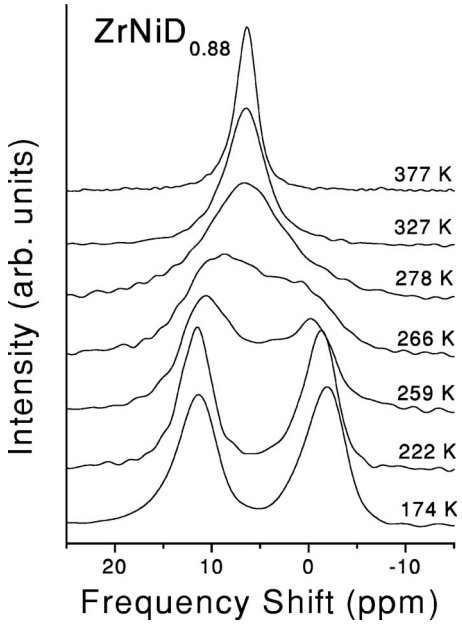

FIG. 5. Temperature dependence of the ^{2}H MAS-NMR spectrum (f_0=76.79 MHz) of $ZrNiD_{0.88}$. As temperature increases, the two β-phase resonances coalesce at 266 K due to the increasing rate of deuterium hopping between the two inequivalent sites in that phase.

The coalescence of the β-phase lines in Fig. 3 makes it possible to see the +7.9 ppm resonance of the γ phase, which appears as a shoulder on the high-frequency side in the 273 K spectrum. Raising the temperature further results in the coalescence of the two γ-phase lines between 273 and 303 K. Here, the 19.6 ppm frequency splitting is equivalent to 605 Hz, giving $\tau_c = 5.3 \times 10^{-4}$ s at ~290 K. The coalescence temperature observed previously[10] in $ZrNiD_{3.0}$ was significantly higher (329 K); thus D motion is slower at a given temperature in the γ phase when x=3.0 compared to $x \approx 2.7$ due to increased site blocking (i.e., fewer Zr_3Ni site vacancies). The slowing of D motion with an increasing concentration in the γ phase was also noted by Browning *et al.*[25] in $ZrNiH_x$ and $ZrNiD_x$.

C. NMR-$ZrNiD_{0.88}$

Figure 4 shows the ^{2}H MAS-NMR spectrum of $ZrNiD_{0.88}$ at 174 K (f_0=76.79 MHz). The spectrum shows two sharp resonances at +11.5 and −1.7 ppm, in good agreement with the β-phase spectrum observed previously[10] in $ZrNiD_{1.0}$. Spinning sidebands are evident at integral multiples of rotor frequency, in this case 6.0 kHz (78.1 ppm). Inversion-recovery spectra (not shown) of $ZrNiD_{0.88}$ at 185 K (with recovery times ranging from 1 ms to 100 s) showed no dependence of the spectrum on recovery time, suggesting that all D atoms are in the same phase with a single value for the spin-lattice relaxation time, T_1=29 s. The shape of both resonances is intermediate between Lorentzian and Gaussian—the slightly Lorentzian tails suggest some local motion is occurring, such as rattling within the site, although hopping between inequivalent sites is frozen out at this temperature. The number of D atoms on each site is proportional to their spectral areas, which was determined by fitting the center line plus the visible sidebands (first and second order) for each resonance using the product of a Gaussian and Lorentzian in each case. Based on the fit (Fig. 4), the ratio of intensities is 1:0.76, as expected for x=0.88 if the energetically preferred site is fully occupied. In this case, the +11.5 ppm line, which shows the larger quadrupole interaction (as indicated by greater intensity in the spinning sidebands), is evidently the energetically preferred site. Hopping between inequivalent sites leads to coalescence of the two lines at 266 K (Fig. 5), confirming that the two lines arise from the same phase. Using Eq. (1), the correlation time τ_c is 3.1×10^{-4} s at 266 K.

D. NMR-$ZrNiD_{2.75}$ and $ZrNiD_{2.99}$ (γ phase)

The temperature dependences of the ^{2}H MAS-NMR spectra (f_0=76.79 MHz) of $ZrNiD_x$ for x=2.75 and x=2.99 are shown in Figs. 6(a) and 6(b), respectively. For $ZrNiD_{2.75}$, the 180 K (rigid-lattice) spectrum (center band plus sidebands) was fit using Lorentzian line shapes as shown in Fig. 6(c). This fit yielded frequency shifts of +9.0 ppm (Zr_3Ni_2 site) and −10.5 ppm (Zr_3Ni site) for the two resonances and a 1:1.8 ratio of intensities, in good agreement with the predicted 1:1.75 ratio, assuming no impurity phases are present. The correlation time for deuterium hopping τ_c is 2.1×10^{-4} s at the coalescence temperature, which is ~270 K.

For the $ZrNiD_{2.99}$ sample, the 213 K (rigid-lattice) spectrum was also fit using Lorentzian line shapes to yield frequency shifts of +9.6 ppm (Zr_3Ni_2 site) and −10.0 ppm (Zr_3Ni site) and a ratio of intensities of 1:2.1, in excellent

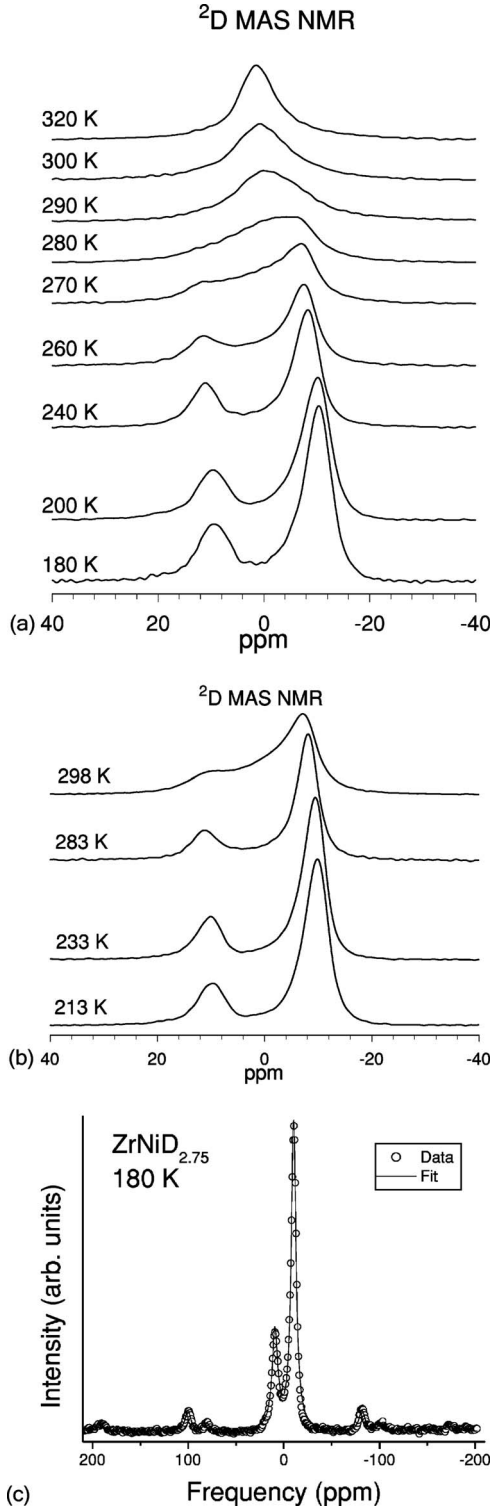

FIG. 6. Temperature dependences of the ^{2}H MAS-NMR spectra (f_0=76.79 MHz) of the γ-phase samples $ZrNiD_{2.75}$ (a) and $ZrNiD_{2.99}$ (b). Coalescence of the lines, due to deuterium hopping, is observed at ~270 K for x=2.75 and ~300 K for x=2.99. (c) A fit of the rigid lattice spectrum for $ZrNiD_{2.75}$ obtained at 180 K.

agreement with the spectral parameters attained previously for x=3.0 at lower field.[10] The hopping correlation time τ_c is 2.1×10^{-4} s at the coalescence temperature, which is ~300 K in this case.

Table II summarizes the ^{2}H MAS-NMR spectral parameters for all $ZrNiD_x$ samples studied in the present work and in Ref. 10. The 19.6 ppm splitting is observed in all γ-phase samples, while the average frequency shift becomes more negative as the concentration in the γ phase is decreased. Measured correlation times for deuterium hopping in $ZrNiD_x$ (from the present work and Refs. 10 and 25) are summarized in Table III and Fig. 7. Browning *et al.*,[25] derived the motional parameters (activation energy E_a and prefactor τ_0) for H motion in $ZrNiH_x$ from measured relaxation times. The temperature dependence of the H correlation times for x =0.88, 2.57, and 2.98, calculated using their parameters, are plotted as straight lines in Fig. 7. Browning *et al.*, further concluded that the motional parameters for D motion in $ZrNiD_x$ are essentially the same as in $ZrNiH_x$ for a given x, based on the correlation times calculated from the ^{2}H T_1 and T_2 minima, although the activation energies derived from their ^{2}H relaxation data differed significantly from those derived from ^{1}H relaxation.[25] Measured correlation times from the present work (coalescence of MAS spectra) and Ref. 10 agree well with the H correlation times and the measured D correlation times of Browning *et al.*, supporting their conclusion that the motional parameters are very similar for the hydrides and deuterides.

E. Neutron vibrational spectra for $ZrNiD_x$ and $ZrNiH_{0.88}$

Figure 8 illustrates the vibrational spectra for $ZrNiD_{0.88}$ and $ZrNiH_{0.88}$ between 10 and 300 K. The 10 K spectrum for $ZrNiD_{0.88}$ displays six distinct peaks at 54.6, 73.5, 78.1, 84.0, 90.8, and 95.3 meV (N.B., 1 meV=8.065 cm^{-1}). Since three normal-mode vibrations should accompany each different deuterium site, this is further evidence that there are two crystallographically distinct deuterium sites in the β-phase structure, not just one site as proposed by Westlake and others.[4,6] The 10 K spectrum for $ZrNiH_{0.88}$ displays an analogous spectral behavior to that of $ZrNiD_{0.88}$, but shifted in energy by roughly a factor of $\sqrt{2}$ due to the half-as-light isotopic mass for H compared to D. Yet, the spectral features for $ZrNiH_{0.88}$ are a little broader than those for $ZrNiD_{0.88}$ and with somewhat different relative peak positions, leading to substantial peak overlap and more difficulty differentiating individual peaks. Nonetheless, the six analogous H peaks appear to be in the vicinity of 75.4, 102, 107.5, 111.5, 121.5, and 128 meV. Raising the temperature toward 300 K causes the spectra for both $ZrNiD_{0.88}$ and $ZrNiH_{0.88}$ to become more attenuated and smeared out. The attenuation reflects the effect of increased D and H Debye-Waller factors with temperature. The apparent spectral smearing reflects the emergence of additional multiphonon scattering on the lower-energy side of the spectral peaks due to a combination of optic-mode excitations with deexcitations of thermally excited acoustic modes.

It is informative to compare the current NVS data with the earlier, lower-resolution data of Benham *et al.*,[8] for $ZrNiH_{0.6}$. The authors concluded that the relatively weak 76 meV feature at 80 K represented a normal-mode vibration with an anomalously large Debye-Waller factor. This is consistent with the relatively larger attenuation observed in Fig. 8 for

TABLE III. Summary of measured deuterium correlation times for $ZrNiD_x$ samples from Ref. 25, Ref. 10, and this study.

Data point	Sample	Phase	$10^3/T$ (K^{-1})	τ_c (s)	Measurement	Source
A	$ZrNiD_{0.87}$	β	2.1	5.5×10^{-9}	T_1 minimum	Ref. 25
B	$ZrNiD_{0.87}$	β	3.8	4.7×10^{-5}	T_2 minimum	Ref. 25
C	$ZrNiD_{0.88}$	β	3.8	3.1×10^{-4}	coalescence	This work
D	$ZrNiD_{1.0}$	β	4.5	7.7×10^{-4}	coalescence	Ref. 10
E	$ZrNiD_{1.0}$	β	3.5	1.4×10^{-4}	defeat of MAS[a]	Ref. 10
F	$ZrNiD_{1.87}$	β	4.4	7.7×10^{-4}	coalescence	This work
G	$ZrNiD_{1.87}$	γ	3.5	5.3×10^{-4}	coalescence	This work
H	$ZrNiD_{2.64}$	γ	1.9	5.5×10^{-9}	T_1 minimum	Ref. 25
I	$ZrNiD_{2.64}$	γ	3.5	4.0×10^{-5}	T_2 minimum	Ref. 25
J	$ZrNiD_{2.75}$	γ	3.7	2.1×10^{-4}	coalescence	This work
K	$ZrNiD_{2.98}$	γ	2.9	4.0×10^{-5}	T_2 minimum	Ref. 25
L	$ZrNiD_{3.0}$	γ	3.0	5.3×10^{-4}	coalescence	Ref. 10
M	$ZrNiD_{2.99}$	γ	3.4	2.1×10^{-4}	coalescence	This work
N	$ZrNiD_{3.0}$	γ	2.6	1.1×10^{-5}	line narrowing	Ref. 10

[a]At the temperature where the hopping rate is roughly the same as the MAS rotor frequency, the random, thermally activated motion partially defeats the coherent averaging due to MAS, resulting in an observable broadening of the MAS spectrum.

this feature for both $ZrNiH_{0.88}$ (at 75.4 meV) and $ZrNiD_{0.88}$ (at 54.6 meV) with increasing temperature compared to the higher-energy modes. Yet, based on their lower-resolution 80 K $ZrNiH_{0.6}$ spectrum (which looked only marginally more resolved than the current 300 K $ZrNiH_{0.88}$ spectrum in Fig. 8), the authors mistakenly concluded that there were only three normal-mode peaks, consistent with a single H site.

Figure 9 compares the 10 K NVS spectra for $ZrNiD_x$ ($x=0.88$, 1.87, 2.50, 2.75, and 3.0). The γ-phase $ZrNiD_3$ spectrum illustrates a multipeak structure consistent with the presence of two crystallographically distinct deuterium sites, as claimed previously.[3,4,6,10] This spectrum shows no traces of a β-phase contribution as indicated by the lack of a β-phase peak at 54.6 meV. In contrast, this β-phase peak is definitely present in the $ZrNiD_{2.50}$ spectrum and a much weaker peak is also seen at 51.7 ± 0.2 meV for $ZrNiD_{2.75}$. However, its $\sim$3 meV shift suggests that this peak may possibly come from the $Zr_9Ni_{11}D_x$ impurity phase (whose vibrational energies are currently unknown) instead of the β phase. On the other hand, the β-phase $ZrNiD_{0.88}$ spectrum shows no traces of a γ-phase contribution as indicated by the lack of a γ-phase peak at 102.2 meV. This observation is consistent with both the MAS-NMR result indicating that $x=0.88$ is single-phase and the XRD result indicating that the maximum stoichiometry for the β phase is 0.90 ± 0.04. Upon comparison of all the NVS spectra in Fig. 9, it is clear that the $ZrNiD_{1.87}$ spectrum is a mixture of both β-phase and γ-phase spectra. This is confirmed by the "β-phase" difference in Fig. 9 produced by subtracting from the $ZrNiD_{1.87}$ spectrum a scaled $ZrNiD_3$ spectrum with 72% of the integrated scattering intensity of the $ZrNiD_{1.87}$ spectrum. The subtraction cannot be expected to be perfect since it assumes that the subtracted γ-phase spectral component of $ZrNiD_{1.87}$ will be the same as the $ZrNiD_3$ spectrum. This assumption is not completely accurate, since NPD results and the MAS-NMR spectrum of $ZrNiD_{1.87}$ presented here indicate that the γ phase in the two-phase region is deuterium-deficient. Nonetheless, the subtraction is reasonably good since it yields a spectrum with only "β-phase" features. This suggests that the β-phase and γ-phase components in the two-phase region, although possessing different deuterium stoichiometries than $ZrNiD_{0.88}$ and $ZrNiD_3$, yield similar vibrational spectra.

Ignoring differences in Debye-Waller factors for deuterium in the two phases, the relative integrated intensities of the β-phase and γ-phase vibrational spectra comprising the $ZrNiD_{1.87}$ spectrum is a measure of the relative number of deuterium atoms associated with each phase. This spectral area analysis estimates that, at 10 K, $72\pm2\%$ of the D atoms in $ZrNiD_{1.87}$ are in the γ phase and $28\pm2\%$ are in the β phase, corresponding to a γ-phase boundary near 3.

F. Neutron-powder diffraction for $ZrNiD_x$

Portions of the neutron-powder-diffraction (NPD) patterns obtained at 295 K for $ZrNiD_x$ ($x=0.0$, 0.88, 1.87, 2.5, 2.75, and 3.0) are shown in Fig. 10. Since the present Rietveld model refinement for $x=3$ is in good agreement with the published structure of Westlake *et al.*,[4,6] this composition will not be discussed further. As mentioned earlier, although the β-phase $ZrNiD_{0.88}$ NPD pattern did not seem to match the previously reported triclinic structure proposed by Westlake,[4,6] we were able to index it successfully over the entire 3–160° measured angular range using a different triclinic unit cell for space group $P1$ (No. 1), which agrees with XRD data on the same sample. Corresponding lattice parameters determined from this NPD pattern are also listed in

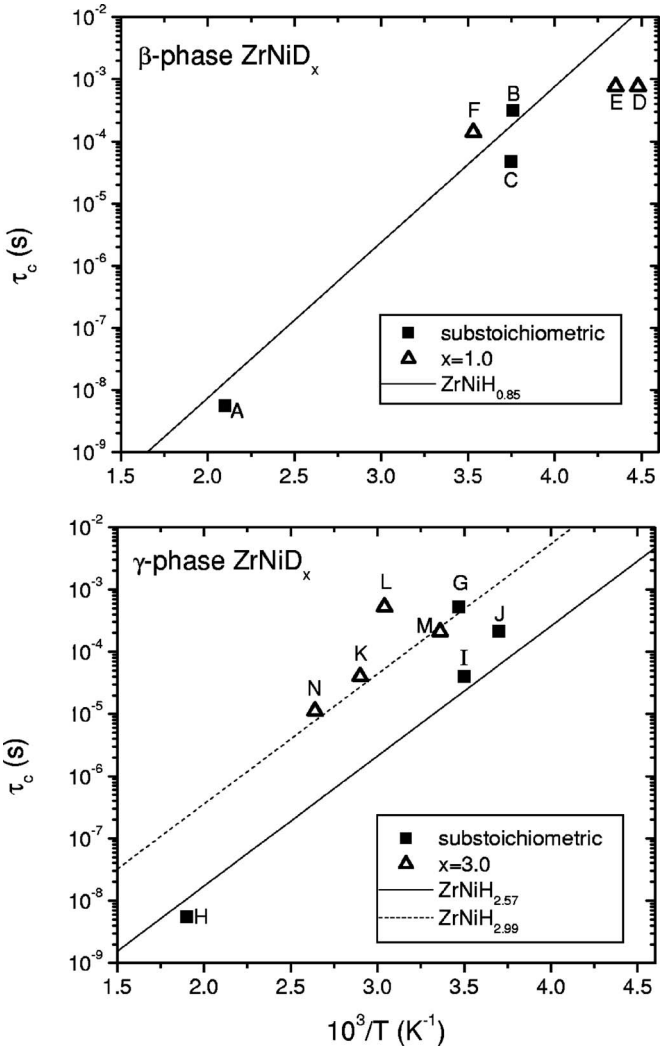

FIG. 7. The data point labels (*A*–*N*) are explained in Table III. Upper: Temperature dependence of measured correlation times for deuterium motion in β-ZrNiD$_x$. The solid line is the temperature dependence of the correlation time for hydrogen motion in ZrNiH$_{0.88}$ calculated using motional parameters determined in Ref. 25. Lower: Temperature dependence of correlation times for deuterium motion in γ-ZrNiD$_x$. The calculated temperature dependence of the correlation time for hydrogen motion in ZrNiH$_x$ is given for $x=2.57$ (solid line) and $x=2.98$ (dotted line), using motional parameters determined in Ref. 25. In both the upper and lower plots, the agreement between the hydrogen and deuterium correlation times indicates that the motional parameters (activation energy and prefactor τ_0) are nearly the same in hydrides and deuterides with similar concentration x.

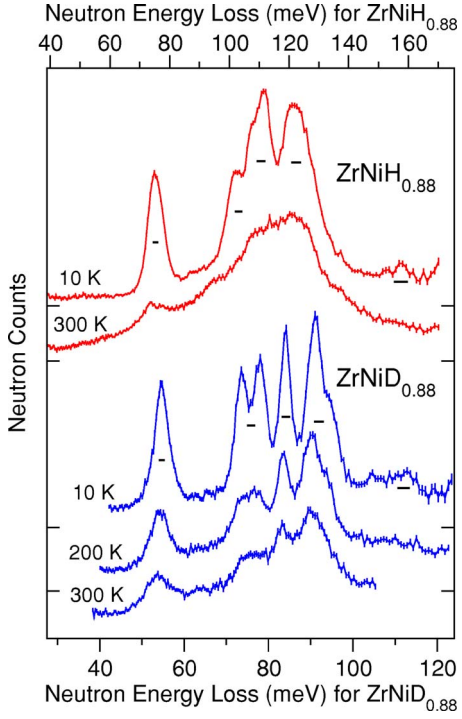

FIG. 8. (Color online) Neutron vibrational spectra for ZrNiH$_{0.88}$ and ZrNiD$_{0.88}$ at various temperatures. For a harmonic comparison, the ratio of corresponding energy-loss scales for hydride and deuteride is $\sqrt{2}$. Spectral sets for each sample are normalized with respect to the ZrNi mass. Normalization between ZrNiD$_{0.88}$ and ZrNiH$_{0.88}$ spectra was chosen to yield comparable peak heights. For clarity, each spectral base line is shifted vertically, the amount designated by horizontal tick marks on the sides of the graph. Instrumental energy resolutions [full width at half maximum (FWHM)] are depicted by the horizontal bars beneath the spectra. Lines through the spectra are intended only as guides to the eye.

Table I and are close to the values obtained from the independent XRD pattern. Due to the low symmetry combined with broadened and distorted peaks in the NPD pattern as well as incompletely resolved contributions from impurity phases such as $Zr_9Ni_{11}D_x$, we were unable to obtain a convergent solution of the β-ZrNiD$_{0.88}$ crystal structure. However, it is hoped that further NPD measurements coupled with Rietveld analysis will eventually be successful in determining the exact crystallographic structure, and thus, the identity of the different deuterium sites observed by NMR and NVS. In agreement with all of the other present results, the NPD pattern for ZrNiD$_{1.87}$ contains comparable amounts of β and γ phases. While some β-phase peaks are evident in ZrNiD$_{2.50}$, they are vanishingly weak or absent for ZrNiD$_{2.75}$, indicating an essentially pure γ phase with some $Zr_9Ni_{11}D_x$ impurity phase.

Figure 11 illustrates the temperature dependence of the γ-phase Zr_3Ni site occupancy for ZrNiD$_{2.75}$ determined by Rietveld refinement fits of the NPD data with the γ-ZrNiD$_x$ structural model, assuming full occupancy of the more stable Zr_3Ni_2 site. At 300 K, the Zr_3Ni site occupancy is ~0.93, which translates to a γ-phase stoichiometry of $x=2.86\pm0.03$, recalling that there are two Zr_3Ni sites and one Zr_3Ni_2 site per formula unit. The site occupancy increases to ~0.965 (which translates to $x=2.93\pm0.02$) as the temperature is decreased to ~170–180 K, then remains constant (i.e., freezes out) as the temperature is decreased further. Since there is no clear sign of β-phase diffraction peaks for this sample stoichiometry, it seems feasible that the change in Zr_3Ni-site occupancy can be enabled by a transfer of D atoms between the γ phase and the $Zr_9Ni_{11}D_x$ impurity phase as well as amorphous and/or nanocrystalline β phase. The Zr_9Ni_{11} impurity phase in the undeuterided ZrNi alloy was confirmed by Rietveld refinement to be of the order of

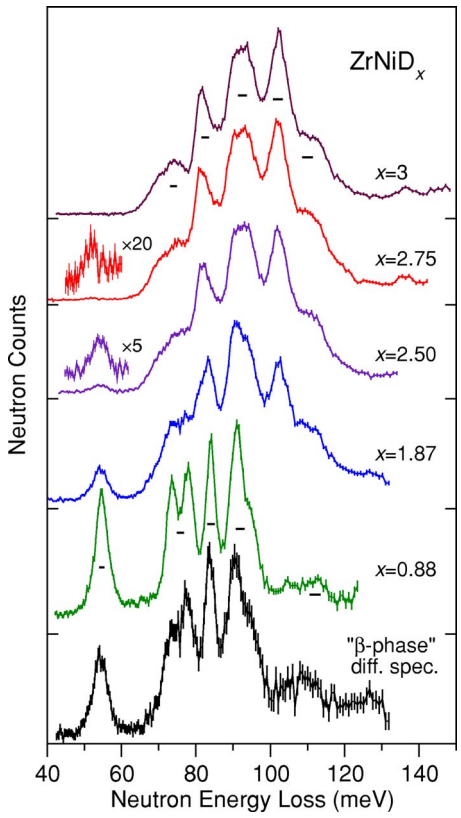

FIG. 9. (Color online) The NVS spectra for $x \geq 0.88$ obtained at 10 K to cover the extremes of the mixed $\beta+\gamma$-phase region. Also plotted at the bottom is the "β-phase" component of $ZrNiD_{1.87}$ derived from the $ZrNiD_{1.87}$ spectrum minus a scaled-down $ZrNiD_{3.0}$ spectrum with 72% of the integrated scattering intensity of the $ZrNiD_{1.87}$ spectrum. Normalization for each plotted spectrum was chosen to yield comparable peak heights. For clarity, each spectral baseline is shifted vertically, the amount designated by horizontal tick marks on the sides of the graph. Instrumental energy resolutions (FWHM) are depicted by the horizontal bars beneath the spectra. Lines through the spectra are intended only as guides to the eye.

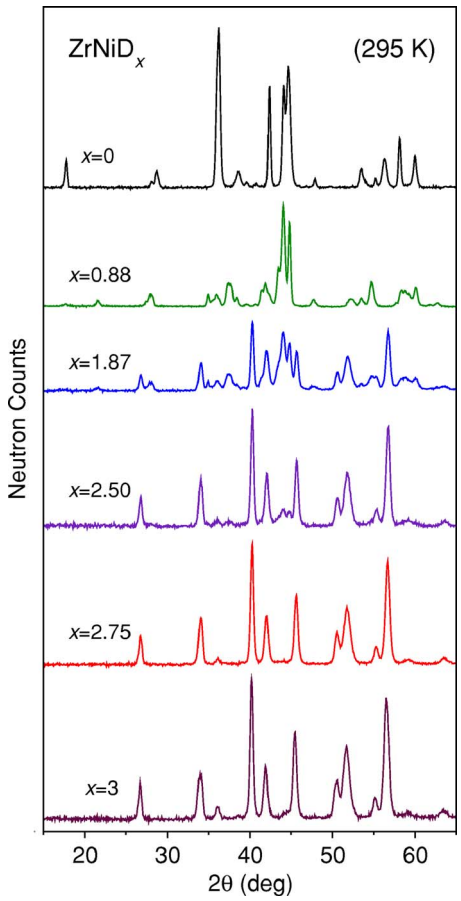

FIG. 10. (Color online) Neutron-powder-diffraction patterns between 15 and 65° 2θ at 295 K for $ZrNiD_x$ (x=0.0, 0.88, 1.87, 2.5, 2.75, and 3.0).

2 wt. %. Since Zr_9Ni_{11} is known to absorb at least ~1D/metal atom,[18,26] a simple calculation indicates that this impurity phase could account for the majority of D atoms needed to change the observed γ-phase Zr_3Ni site occupancy without a noticeable formation or depletion of a β phase.

The γ-phase stoichiometry of $x=2.93\pm0.02$ determined from these NPD data for T=10–180 K implies that 75±2% of the D atoms belong to the $ZrNiD_{1.87}$ γ phase, assuming the β-phase stoichiometry is 0.90±0.04. The fraction of D atoms in the γ phase estimated from NVS at 10 K (72±2%) and MAS-NMR at 163 K (78±5%) are therefore in reasonable agreement with the more reliable NPD result.

The temperature dependence of the Zr_3Ni site occupancy is also reflected in the anomalous lattice parameter and unit-cell-volume behavior between 10 and 300 K in Fig. 11. As the temperature is decreased from 300 to 180 K, the c lattice parameter remains unchanged until ~270 K then increases with increasing site occupancy, reaching a maximum value where the occupation begins to freeze out at ~180 K. Decreasing the temperature below 180 K, where the occupation now remains constant, leads to a more normal resumption of thermal contraction in the c lattice parameter. The a lattice parameter remains largely unchanged between 300 and 150 K, and undergoes a more normal thermal contraction below 150 K. In contrast to a and c, the b lattice parameter decays monotonically with decreasing temperature over the whole range. The odd unit-cell-volume behavior results from the combined temperature dependences of the three lattice parameters. It is not clear at present to what extent these effects are also associated with some type of ordering of the D atoms within the γ phase. The ^2H MAS-NMR spectra in Fig. 6(a) for $ZrNiD_{2.75}$ do reveal some subtle differences between the 240 K spectrum and the 180 K spectrum (i.e., the low-frequency peak is broadening and beginning to shift toward higher frequency by 240 K) indicating that some diffusion motion is occurring, but it is just not fast enough to cause coalescence of the peaks until the temperature is greater than ~260 K. In fact, the spectrum is not fully rigid on the NMR time scale until ~200 K or even 180 K where diffusion probably has not fully ceased—it is only too slow to be detected from these NMR experiments. Hence, NMR generally corroborates that some type of slow diffusion process occurs within the γ phase over the temperature range (~180–300 K) where the lattice parameters are also exhibiting unusual behavior. It was not possible to demonstrate if ordering is involved.

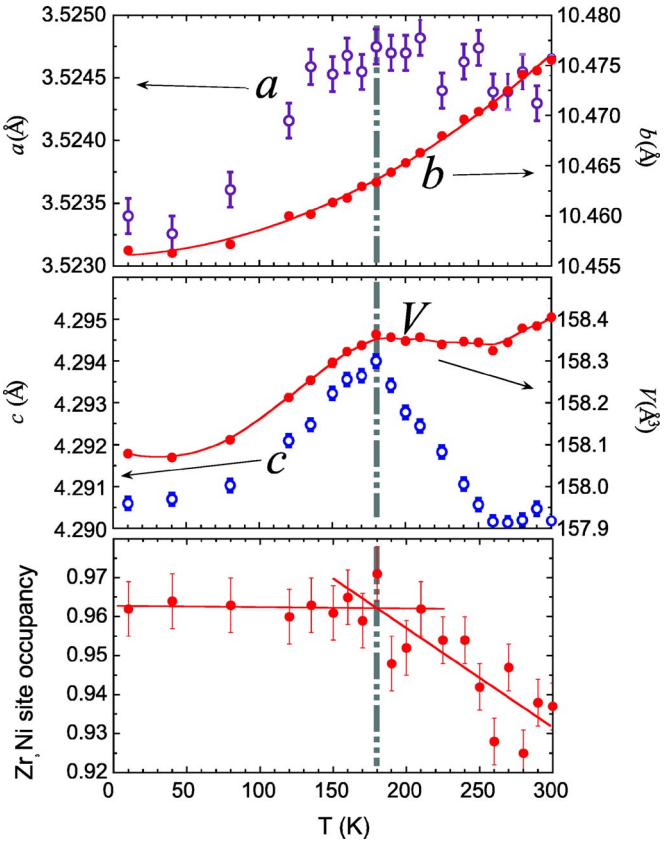

FIG. 11. (Color online) Temperature dependences of the γ-phase lattice parameters, unit-cell volume, and Zr_3Ni deuterium-site occupancies for $ZrNiD_{2.75}$ obtained from NPD measurements. The vertical bar denotes the boundary between the normal behavior observed at lower temperatures and the unusual effects described in the text above ~180 K.

IV. SUMMARY AND CONCLUSIONS

The present XRD, NMR, and NPD results indicate that $ZrNiD_{0.88}$ is essentially composed of the β phase, but with a triclinic lattice much more distorted than was indicated by Westlake.[4,6] XRD measurements of $ZrNiD_{1.0}$ reveal that 5 ± 1 % of metal atoms are in the γ phase at this composition, indicating that the upper β-phase boundary is $x=0.90\pm0.04$.

For $ZrNiD_{1.87}$, the XRD patterns, ^{2}H MAS-NMR spectra, NVS, and NPD results presented here show that two phases (β and γ) are present. The NPD results indicate a lower γ-phase boundary of $x=2.86\pm0.03$ near room temperature, which increases to 2.93 ± 0.02 at temperatures below ~180 K, higher than the phase boundaries determined from previously reported isotherms at $T>330$ K.[11–16] These results suggest that the γ-phase boundary is more strongly temperature-dependent than previously believed.[5]

NVS and MAS-NMR spectra of $ZrNiD_{0.88}$ demonstrate that two inequivalent D sites are occupied in the β phase. Furthermore, NVS and MAS-NMR spectra of $ZrNiD_{1.87}$ demonstrate these two sites are definitely not the Zr_3Ni and Zr_3Ni_2 sites occupied in the γ phase, as was suggested by two previous studies of samples with $x<1$.[8,9] All the NVS spectra for $x\geq0.88$ clearly show different symmetry for the two sites in the β phase compared to those occupied in the γ phase, while the NMR spectra show different frequencies and line shapes for the β-phase lines compared to the γ-phase lines. We tentatively suggest that the two inequivalent sites in the triclinic β phase are both nominally Zr_4Ni_2 sites, which have been rendered inequivalent by the triclinic distortion of the host lattice. In the orthorhombic lattice, all Zr_4Ni_2 sites are equivalent, but the Zr_4Ni_2 sites take on two slightly different shapes in the triclinic lattice. Thus, the H(D) atoms may sit in slightly different positions relative to the metal atoms within the two classes of Zr_4Ni_2 sites, resulting in different site energies observed in NVS experiments and different Knight shifts observed in the NMR spectra. This picture explains the present observation of two inequivalent occupied sites in β-phase $ZrNiD_x$, even though previous theoretical considerations predicted that a single Zr_4Ni_2 site would be most stable (assuming orthorhombic *Cmcm* symmetry)[6,9,16,17] and prior experiments[3,4] indicated that only this Zr_4Ni_2 site is occupied in the $ZrNi(H/D)_x$ β phase. However, when temperatures are >300 K, the diffusive motions may be rapid enough to result in an averaged occupancy obscuring these observed differences in site behavior. Unfortunately, NPD has yet to clear up the confusion concerning site occupancies. The combination of the low-symmetry triclinic structure and extensive peak overlaps in the NPD pattern for the current β-$ZrNiD_{0.88}$ sample have so far precluded a converged solution of the crystal structure with acceptable residual errors. Additional samples are being prepared for future NPD measurements that, along with more detailed analyses, may finally shed light on the true crystal structure and thus the locations of these sites in the β phase. Correlation times for deuterium hopping between inequivalent sites were determined from the temperature dependence of the ^{2}H MAS-NMR spectrum and are consistent with motional parameters for $ZrNiH_x$ determined previously by ^{1}H NMR,[25] suggesting that there is no significant difference in the motion of the different isotopes.

ACKNOWLEDGMENTS

The authors appreciate helpful conversations with M. S. Conradi and also the assistance of M. Prina with the preparation of some of the $ZrNi(H/D)_x$ samples at JPL. N.L.A. gratefully acknowledges support from Research Corporation (Grant No. CC4705) and the NSF (Grant No. DMR-9804094). This research was partially performed at the Jet Propulsion Laboratory, California Institute of Technology, under a contract with the National Aeronautical and Space Administration. The NMR facility at Caltech was supported by the National Science Foundation under Grant No. 9724240 and partially supported by the MRSEC Program of the National Science Foundation under Grant No. DMR-0080065.

*Please correspond with Robert Bowman at JPL Mail Stop 79-24. FAX: 1-818-393-4878. Electronic address: robert.c.bowman-jr@jpl.nasa.gov

[1] G. G. Libowitz, H. F. Hayes, and T. R. P. Gibb, Jr., J. Phys. Chem. **62**, 76 (1958).
[2] W. L. Korst, J. Phys. Chem. **66**, 370 (1962).
[3] S. W. Peterson, V. N. Sadana, and W. L. Korst, J. Phys. (Paris) **25**, 451 (1964).
[4] D. G. Westlake, H. Shaked, P. R. Mason, B. R. McCart, M. H. Mueller, T. Matsumoto, and M. Amano, J. Less-Common Met. **88**, 17 (1982).
[5] R. Kronski and T. Schober, J. Alloys Compd. **205**, 175 (1994).
[6] D. G. Westlake, J. Less-Common Met. **75**, 177 (1980).
[7] I. Jacob and J. M. Bloch, Solid State Commun. **42**, 541 (1982).
[8] M. J. Benham, J. D. Browne, and D. K. Ross, J. Less-Common Met. **103**, 71 (1984).
[9] S. Yang, F. Aubertin, P. Rehnbein, and U. Gonser, Z. Kristallogr. **195**, 281 (1991).
[10] N. L. Adolphi, S. Badola, L. A. Browder, and R. C. Bowman, Jr., Phys. Rev. B **65**, 024301 (2001); N. L. Adolphi, S. Badola, L. A. Browder, and R. C. Bowman, Jr., *ibid.* **69**, 149901(E) (2004).
[11] W. Luo, A. Craft, T. Kuji, H. S. Chung, and T. B. Flanagan, J. Less-Common Met. **162**, 251 (1990).
[12] K. Watanabe, K. Tanaka, M. Matsuyama, and K. Hasegawa, Fusion Eng. Des. **18**, 27 (1991).
[13] J. S. Cantrell, R. C. Bowman, Jr., L. A. Wade, S. Luo, J. S. Clewley, and T. B. Flanagan, J. Alloys Compd. **231**, 518 (1995).
[14] P. Dantzer and P. Millet, Rev. Sci. Instrum. **71**, 142 (2000).
[15] P. Dantzer, P. Millet, and T. B. Flanagan, Metall. Mater. Trans. A **32A**, 29 (2001).
[16] N. Michel, S. Poulat, P. Millet, P. Dantzer, L. Priester, and M. Gupta, J. Alloys Compd. **330-332**, 280 (2002).
[17] M. Gupta, J. Alloys Compd. **293-295**, 190 (1999).
[18] K. Watanabe, M. Hara, M. Matsuyama, I. Kanesaka, and T. Kabutomori, Fusion Technol. **28**, 1437 (1995).
[19] T. Kabutomori, Y. Wakisaka, K. Tsuchiya, and H. Kawamura, J. Nucl. Mater. **258-263**, 481 (1998).
[20] B. D. Freeman, E. L. Ryba, R. C. Bowman, Jr., and J. R. Phillips, Int. J. Hydrogen Energy **22**, 1125 (1997).
[21] R. C. Bowman, Jr., J. Alloys Compd. **356-357**, 789 (2003).
[22] M. Prina, R. C. Bowman, Jr., and J. G. Kulleck, J. Alloys Compd. **373**, 104 (2004).
[23] S. J. C. Irvine, D. K. Ross, I. R. Harris, and J. D. Browne, J. Phys. F: Met. Phys. **14**, 2881 (1984).
[24] Certain commercial suppliers are identified in this paper to foster understanding.
[25] C. D. Browning, T. M. Ivancic, R. C. Bowman, Jr., and M. S. Conradi, Phys. Rev. B **73**, 134113 (2006).
[26] J. M. Joubert, M. Latroche, and A. Percheron-Guegan, J. Alloys Compd. **231**, 494 (1995).
[27] N. L. Adolphi, J. J. Balbach, M. S. Conradi, J. T. Markert, R. M. Cotts, and P. Vajda, Phys. Rev. B **53**, 15054 (1996).
[28] W. T. Dixon, J. Chem. Phys. **77**, 1800 (1982).
[29] A. Bielecki and D. P. Burum, J. Magn. Reson., Ser. A **116**, 215 (1995).
[30] G. Neue and C. Dybowski, Solid State Nucl. Magn. Reson. **7**, 333 (1997).
[31] T. J. Udovic, D. A. Neumann, J. Leão, and C. M. Brown, Nucl. Instrum. Methods Phys. Res. A **517**, 189 (2004).
[32] J. K. Stalick, E. Prince, A. Santoro, I. G. Schroder, and J. J. Rush, in Neutron Scattering in Materials Science II, edited by D. A. Neumann, T. P. Russell, and B. J. Wuensch, MRS Symposia Proceedings Vol. 376 (Materials Research Society, Pittsburgh, 1995), p. 101.
[33] H. M. Rietveld, J. Appl. Crystallogr. **2**, 65 (1969).
[34] A. C. Larson and R. B. Von Dreele, General Structure Analysis System, Los Alamos National Laboratory Report No. LAUR 86-748, 2000.